(Received 14 January 2025, Accepted 3 March 2025, Scheduled 31 March 2025)

Design of an Efficient SRR Loaded Polarization-Independent Wideband Metamaterial Notched Absorber with Wide Reflecting Band for Low Insertion Loss

Abhinav Kumar[1, 2, *] and Jayanta Ghosh[2]

[1] *ECE Department, Bhagalpur College of Engineering, Bihar, India*
[2] *ECE Department, National Institute of Technology, Patna, India*

ABSTRACT: This research introduces a new, compact, absorptive frequency-selective reflector, or notched absorber (AFSR), which is low-profile and polarization-insensitive. The objective of the proposed study is to create a miniaturized FSS-based notched absorber that exhibits a high level of angular stability and a robust operational bandwidth of 110% (4.1 to 14.1 GHz). It consists of a reflecting band situated between two absorption bands. The absorption bands are 4.1 to 5.7 GHz and 9.0 to 14.1 GHz, respectively. A low insertion loss of 0.40 dB is achieved at approximately 6.8 GHz, and a wide reflection window with a -3 dB band is extended from 5.8 GHz to 8.0 GHz. The proposed notched absorber comprises three layers with a metal sheet at the bottom. The intermediate layer serves as a band-pass filter, which passes the in-band signal while working as a ground plane for out-of-band absorption. In contrast, the top layer is responsible for broad out-of-band absorption. The total thickness of the band notch absorber is 0.36λ (where λ stands for the wavelength associated with the lowest operating frequency). The equivalent circuit model of the proposed structure has been developed to understand better how band-notch absorbers work at their most basic level. In addition, we examined the distribution of surface current. The notched absorber that was designed is fabricated, and measurements have been done in a semi-anechoic chamber. The measured results are in excellent agreement with the simulated ones. The proposed notched absorber can be employed in radomes, to reduce electromagnetic interference and protect sensitive equipment from unwanted electromagnetic radiation, superstratum on an antenna, RCS reduction and stealth characteristics.

1. INTRODUCTION

Absorbers are frequency-selective surfaces that absorb incoming electromagnetic waves. They are commonly used in stealth technology, reducing RCS, in radomes, for electromagnetic shielding, and in numerous other applications to limit or selectively lower the reflection or transmission of electromagnetic waves. In 1952, Salisbury [1] proposed the first absorber with a quarter-wavelength thickness, marking the beginning of research on absorbers. This absorber utilises the $\lambda/2$ path difference between the incident wave and the absorber. Destructive interference at the absorber's interface, caused by the $\lambda/2$ path difference between the incoming waves and those that reflect them, cancels out waves.

Salisbury screen suffers from limited bandwidth, so enhancing the multilayer absorber structure (jaumann absorber [2]) is implemented; however, it leads to an increased thickness of the absorber. The wedge-tapered absorber [3] that was proposed in 1971 demonstrated the highest absorption rate, despite its cumbersome structure.

The primary demand for absorbers is stronger absorption effects, wider bandwidth, slimmer, and lighter structures.

Many investigations have been conducted to improve the all-round performance of the absorbers. Multi-resonant structures are implemented to achieve wideband absorption; a combination of resonators tuned to various frequencies can be used. Multiple absorption peaks are possible with this approach and collectively span a wide frequency range [4, 5]. Better impedance matching over a wide frequency range is made possible by gradient-index metamaterials, which gradually switch from one impedance to another. The bandwidth of metamaterial absorbers (MMAs) can be greatly increased using this design approach [6, 7]. To increase the absorption bandwidth, the thickness of the dielectric substrate supports should be increased. However, a larger absorber's total size is the trade-off. An important trade-off in the wideband MMA design is optimizing thickness [8]. Using resistive materials such as resistive sheets, lump resistors, and resistive inks [9], frequency selective surface (FSS)-based microwave absorbers can be designed to absorb a broad spectrum of frequencies. But with this type of FSS, there is no scope for communication.

At the same time, it is important to allow electromagnetic waves to pass through the radomes in the operation band in specific application scenarios, such as radomes, without compromising the absorption and radiation performance of the antennas. Frequency selective rasorbers (FSRs) are specific varieties of FSSs that produce a transmission window between two absorption bands [10, 11]. In certain applications, it is necessary

* Corresponding author: Abhinav Kumar (abhinavk.phd19.ece@nitp.ac.in).

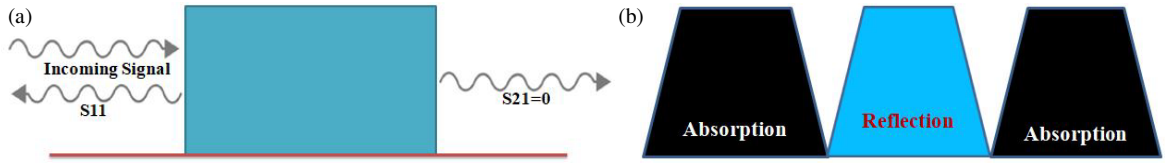

FIGURE 1. Absorption and reflection phenomena of the notched absorber. (a) Notched black box. (b) A-R-A frequency response.

to enhance the radiation efficacy. To achieve this, we employ an absorptive frequency-selective reflector.

The notched absorber is a unique type of FSS that absorbs electromagnetic waves from both sides of the reflection window within a specific frequency range. In addition, notched absorbers or absorptive frequency-selective reflectors (AFSRs) [12, 13] can be utilised as the ground plane for antennas and function as a frequency-selective surface (FSS) reflector. These absorbers are specifically developed to achieve antennas with low radar cross section (RCS) [14].

The objective of the research is to design a miniaturized, wide-reflecting window dual-polarized notched absorber. The proposed notched absorber boasts a relatively high fractional bandwidth, as well as a low insertion loss and improved angular stability. The symmetrical design of the structure renders it insensitive to polarization. The incorporation of notched absorbers not only reduces RCS but also mitigates the interference effects of the co-located radar system, as they function as a substrate when being used as a ground plane for the antenna. The structural electrical equivalent circuit is developed using Advanced Design System (ADS) software to enhance our comprehension of its physical operation. Finally, we fabricate the proposed notched absorber using printed circuit board (PCB) technology and measure it in a semi-anechoic chamber using a vector network analyser (VNA). The simulated results are in excellent agreement with the measured ones.

2. THEORETICAL BACKGROUND

The notched absorber comprises three layers. The upper layer is responsible for the absorption of the signal; the middle layer is used for the proper frequency selective reflective band; and the bottom layer is used for the ground plane for the reflection phenomena. For an ideal notched absorber, the reflection coefficient $(S_{11} = 0)$ and transmission coefficient $(S_{21} = 0)$ for absorption phenomena and $(S_{11} = 1)$ and $(S_{21} = 0)$ for reflection phenomena are calculated by Equation (1) [15].

$$A(\omega) = 1 - |S_{11}|^2 - |S_{21}|^2 \tag{1}$$

where $A(\omega)$, $|S_{11}|^2$, and $|S_{21}|^2$ are absorption, reflected power, and transmitted power respectively, but the notched absorber phenomena are different from absorber as shown in Figure 1.

The overall frequency regime of the notched absorber can be divided into three parts, i.e., lower absorption band (f_1), reflection window (f_2), and upper absorption band (f_3).

For an ideal notched absorber at f_1 and f_3, S_{11} and S_{21} should be zero, and at f_2, S_{21} should be zero, and $S_{11} = 1$.

The notched absorber, as illustrated in Figure 2, has been intelligently designed to produce these phenomena. Specifically,

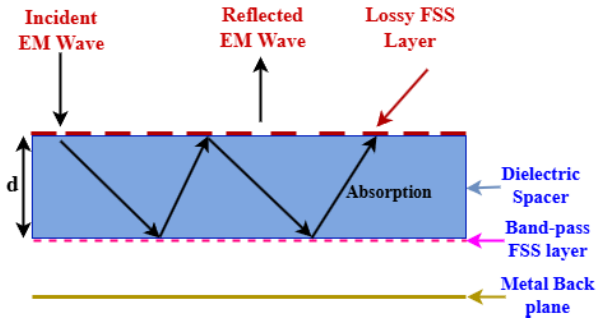

FIGURE 2. Absorption and reflection phenomena based on parallel plate waveguide of the notched absorber.

the structure functions as an absorber when the impedance of the upper layer is equal to the free-space impedance, and the middle layer is zero. To obtain a selective reflective window, the upper and middle layers must resonate simultaneously.

3. UNIT CELL GEOMETRY

The geometry of the unit cell in the proposed notched absorber comprises three distinct layers. To obtain the top layer, a modified split ring resonator is affixed to an FR4 substrate with dielectric loss tangent and permittivity of 0.02 and 4.4, respectively, which functions as a parallel L_2-C_2 resonator circuit. One finger of the split ring functions as an inductor, while the coupling between the fingers functions as a capacitor in parallel with the inductor.

In order to achieve wide out-of-band operation, four chip resistors $(R = 350\,\Omega)$ were incorporated into each unit cell between the circular ring resonators to function as a series circuit R_1-L_1, as illustrated in Figure 10.

Once the top layer is designed, we need to design a middle layer that functions as a band-pass filter, which works as a ground plane for the out-of-band operations and selective transmission for the reflection window. To achieve band-pass filter functionality, slots are carved into the rectangular portion kept in FR4 that functions as parallel L_3-C_3 (bottom layer) resonators to resonate at the same frequency during the selective reflective window as the L_2-C_2 (top layer) resonator circuit. The gap between different layers of the proposed design is separated by foam as an air spacer, which is characterized by a refractive index close to that of air. To create a selective reflection window between two absorption bands, a metal sheet is incorporated at the bottom of the structure. The bottom layer metal sheet reflects the incoming waves that pass through the upper and middle layers. The composite and side views of the unit cell design are shown in Figure 3.

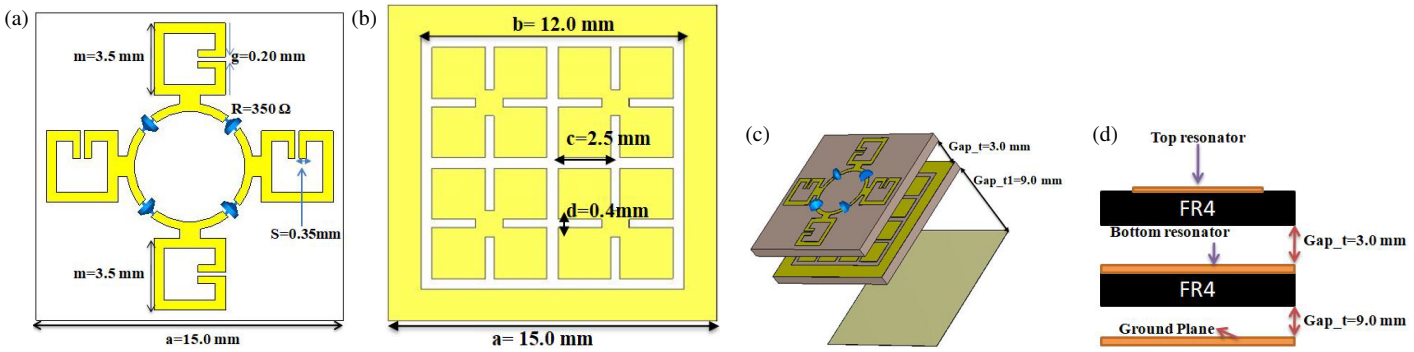

FIGURE 3. Proposed notched absorber unit cell structure. (a) Top layer. (b) Bottom layer. (c) Composite view. (d) Side view of the rasorber.

The air gap is smartly adjusted to get out-of-band absorption and in-band reflection. The optimal parameter of the proposed notched absorber is as follows: $a = 15\,\text{mm}$, $b = 12\,\text{mm}$, $m = 3.5\,\text{mm}$, $Gap\_t = 3.0\,\text{mm}$, and $Gap\_t1 = 9.0\,\text{mm}$.

4. DESIGN EVOLUTION

As mentioned before, the top layer is responsible for the wide out-of-band absorption. On the other hand, the middle layer was designed for the selective reflection window. Figure 4(a) shows that the insertion loss of the reflective window is high, and the out-of-band absorption bandwidth is low.

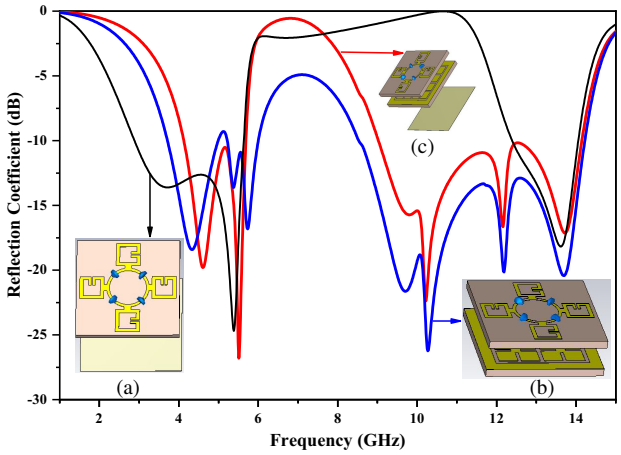

FIGURE 4. Design evolution of the proposed notched absorber.

We incorporate the middle layer, as illustrated in Figure 4(b), to enhance the absorption bandwidth. However, the insertion loss increases due to the electromagnetic (EM) wave's leakage to the opposite side. To overcome this issue, we employed a ground plane at the bottom, as illustrated in Figure 4(c), which prevents the signal from passing through it.

5. PARAMETRIC STUDY

The performance analysis with different values of the structural dimensions is visualized with different parametric studies.

5.1. Effect of Distance between the Top and Middle Resonator

The air gap between the top and middle layer is adjusted in such a way that the middle layer acts as a ground plane for the out-of-band operation and behaves as a band-pass selective filter to get selective reflection for the in-band operation.

During the out-of-band operation when the signal is reflected from the middle layer, it becomes again reflected from the top layer, and these phenomena occur between the top and middle layers multiple times to absorb the out-of-band signal and pass the in-band signal to achieve a reflection window between two absorption bands with a little insertion loss introduced due to finite loss tangent of the top and middle layers. To get the above-mentioned design, we have adjusted the air gap between the top and middle layers (Gap_t) from 2.0 mm to 4.0 mm. The optimum reflection coefficient found at $t_{air} = 3.0\,\text{mm}$ is shown in Figure 5.

5.2. Effect of Chip Resistor

The chip resistors are responsible for wide-band absorption in out-of-band operation. The values of chip resistors vary from $R = 300\,\Omega$ to $R = 400\,\Omega$ to get optimum response at $R = 350\,\Omega$ as shown in Figure 6.

We can observe from Figure 6 that chip resistors are responsible for only wideband absorption in the out-of-band regimes, and the in-band reflection behaviour is unaffected by the chip resistors. At the reflection window at around 6.8 GHz, the parallel L_2-C_2 resonating circuit, formed by the top layer of the notched absorber, resonates and leads to a high impedance of the top layer, as shown in Figure 9. As a result, the surface current distribution is very low across the chip resistors around 6.8 GHz, as shown in Figure 7(b). It indicates that the electromagnetic wave passes through the top layer without any loss. A very small loss is introduced due to the non-zero loss tangent of the top layer FR4 dielectric material.

At the absorption frequency on both sides of the reflection window, due to the non-resonating behaviour of the parallel L_2-C_2 resonator, large surface current flows through the chip resistor as shown in Figure 7(a), which indicates that while the wave passes at these frequencies, losses are introduced due to chip resistors.

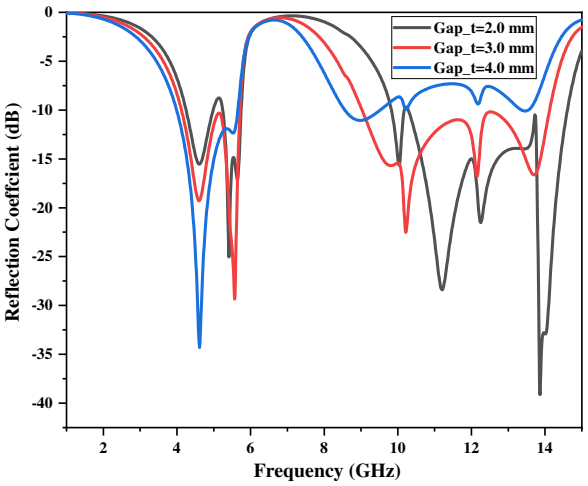

FIGURE 5. Reflection coefficient of the proposed notched absorber for different values of air-gap between the top and middle layer.

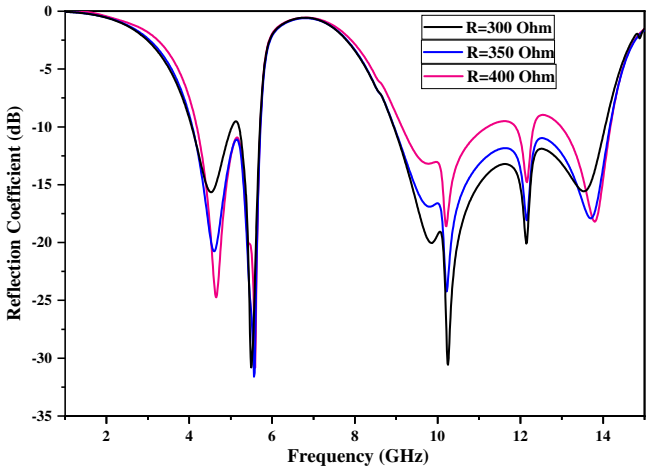

FIGURE 6. Reflection coefficient of the proposed notched absorber for different values of chip resistance.

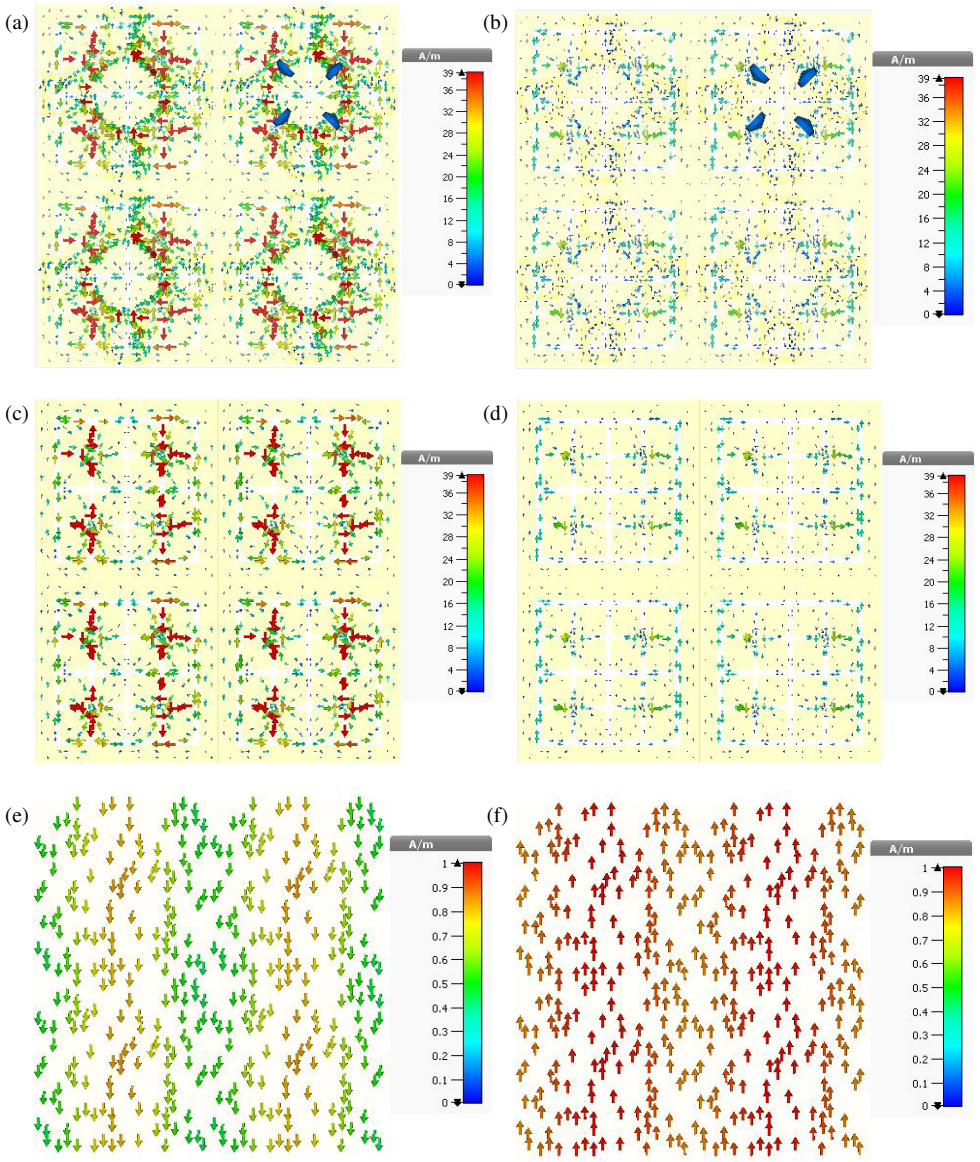

FIGURE 7. Simulated surface current density of the proposed notched absorber at the all the three layers, (a), (c), (e) at 12.0 GHz, (b), (d), (f) at 6.7 GHz.

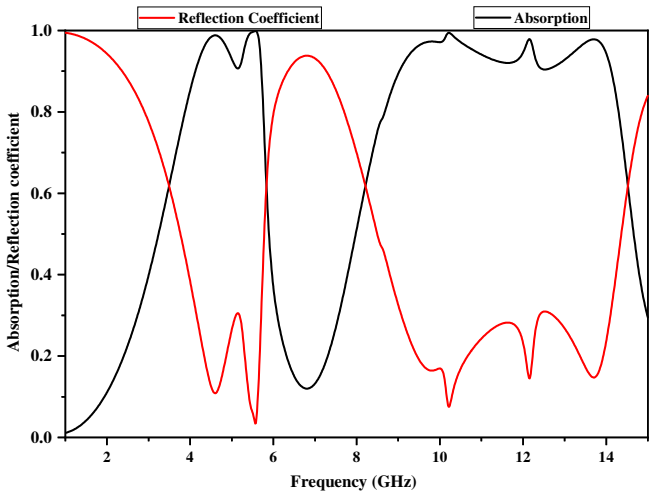

FIGURE 8. Simulated absorption and reflection coefficient for the proposed notched absorber.

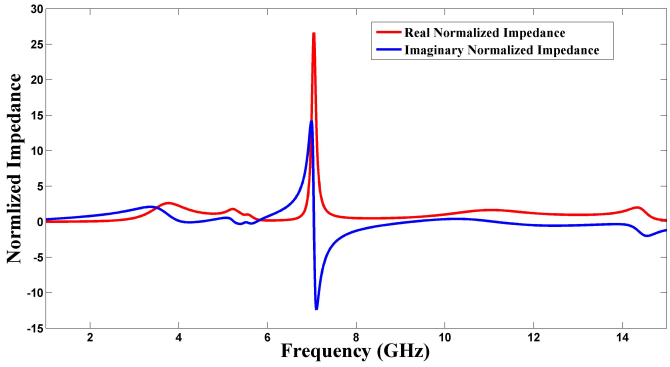

FIGURE 9. Simulated normalized impedance of the proposed notched absorber.

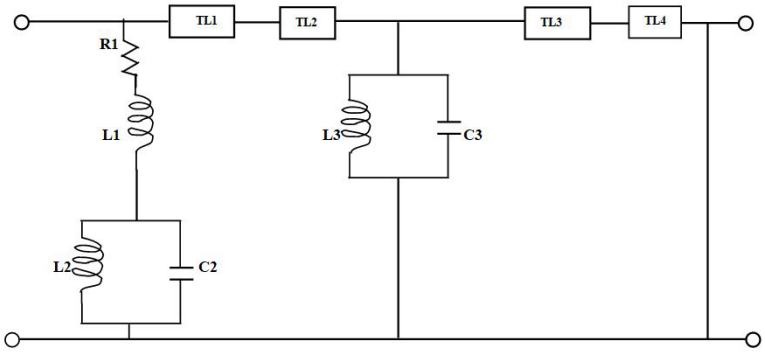

FIGURE 10. Effective equivalent circuit model of the proposed notched absorber.

6. ABSORPTION/REFLECTION PHENOMENA

The out-of-band absorption and in-band reflection obtained from simulation for the proposed notched absorber are depicted in Figure 8. The response provides insights into the frequency response and effectiveness of the notched absorber regarding absorption and reflection coefficient across a specified range. The proposed notched absorber demonstrates its functional range from 4.1 GHz to 14.1 GHz, indicating that it exhibits the desired behavior of selective reflection and absorption within the aforementioned band. The proposed design exhibits two distinct absorption bands, each achieving a minimum of 90% absorption, demonstrating its effectiveness in filtering specific frequency ranges. The first absorption band extends from 4.1 to 5.7 GHz, and the second absorption band spans from 9.0 to 14.1 GHz. Between these two absorption bands, a reflection window is observed near 6.8 GHz. The response of the design notched absorber shows a wide -3 dB reflection window of 2.2 GHz with an insertion loss of just 0.40 dB.

To understand the physical insight of the proposed notched absorber, we have made an electrical equivalent circuit model as illustrated in Figure 10. Different dielectric layers and air spaces between them act as transmission lines.

During in-band selective reflection operation, the parallel L_2-C_2 circuit of the top layer resonates with the EM waves incident on the design structure. This results in high impedance of the top layer around the selective reflection window, as illustrated in Figure 9, and as a result, a very low surface current flows across the chip resistors, as illustrated in Figure 7(b), which demonstrates that the EM wave passes through the top layer without lumped element-introduced loss at these frequencies. However, during the process, a small loss is introduced due to the finite loss tangent of the FR4 dielectric material. The L_3-C_3 resonating circuit of the middle layer resonates when EM waves reach the middle layer, acting as a selective bandpass filter, and these waves are reflected back to the incident side as bottom layer functions as a reflector, as illustrated in Figure 7. At port 1, we receive these reflected waves as an in-band reflection window around 6.8 GHz.

During out-of-band absorption on both sides of the in-band reflection, the normalized impedance of the top layer is matched to the free space impedance in the desired frequency range shown in Figure 9 due to which EM waves enter the structure with very low reflection but non-resonating behaviour of the top layer parallel L_2-C_2 circuit, and the surface current across the chip resistor increases drastically which is shown in the Figure 7(a), indicating that EM waves lose some of their energy through chip resistors while passing through the top layer. When EM waves reach the middle layer, the gap

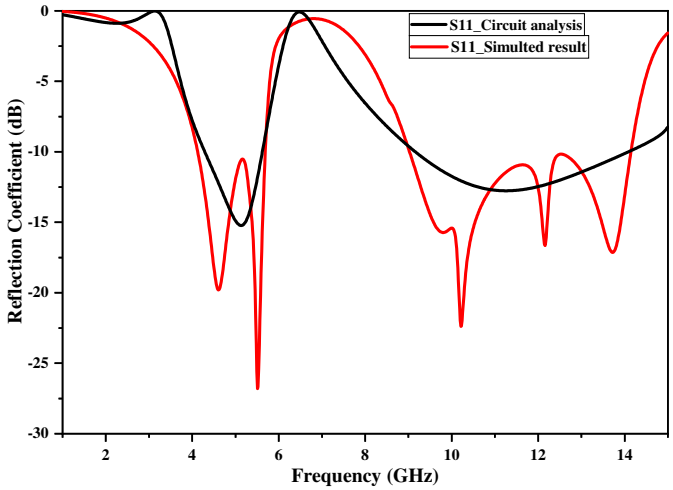

FIGURE 11. Comparison of simulated and equivalent circuit analysis of the proposed notched absorber.

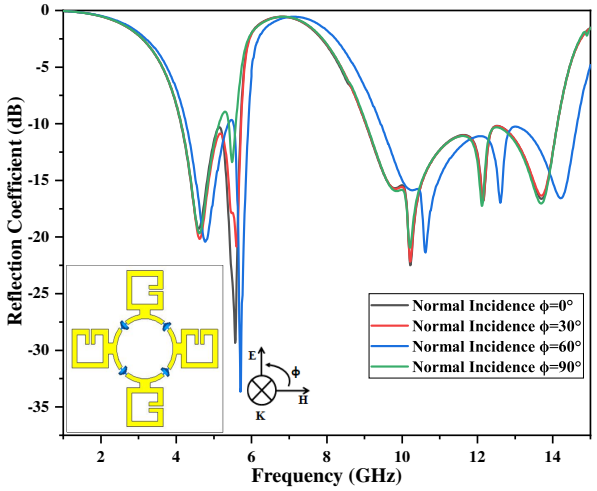

FIGURE 12. Simulated reflection coefficient for the proposed notched absorber for different polarization angles.

TABLE 1. Experimental and simulation results of the proposed rasorber.

Simulated Notched Absorber				Measured Notched Absorber			
Out-of-Band Absorption		In-Band Reflection Window		Out-of-Band Absorption		In-Band Reflection Window	
Absorption	BW	Transmission window	IL	Absorption	BW	Transmission window	IL
More than 80%	4.1 to 14.1 GHz 10.0 GHz	6.8 GHz	0.4 dB	More than 80%	4.0 to 13.8 GHz 9.8 GHz	6.75 GHz	0.45 dB

of this layer is then excited to act as a ground plane which is shown in Figure 7(c) with surface current high near the gap. As the middle layer acts as a ground plane for the out-of-band operation, EM waves are reflected and bounced between the top and middle layers multiple times to absorb the signal.

By setting the initial set of lumped element values to the best values, it is possible to get responses that are very similar between the electromagnetic simulation done with Advanced Design System (ADS) and the simulation done with CST Microwave Studio [16]. For the maximal absorption and reflection window bandwidth, the lumped elements' final values are as follows: $R1 = 235.0\,\Omega$, $L1 = 0.001\,\text{nH}$, $L2 = 4.6\,\text{nH}$, $C2 = 0.56\,\text{pF}$, $L3 = 33\,\text{nH}$, and $C3 = 0.54\,\text{pF}$. The reflection coefficient from the circuit simulation is compared to that obtained from the full-wave analysis, and the results are in good accord, as illustrated in Figure 11. This confirms the equivalent circuit of the proposed notched absorber.

7. POLARIZATION-INSENSITIVE BEHAVIOR

7.1. Normal Incidence Results

To evaluate the polarization behavior of the proposed notched absorber, a test was conducted where the direction of electromagnetic wave propagation remained constant while the orientations of the electric and magnetic fields were rotated, changing the polarization angle (ϕ) incremented by 30°. The experiment aimed to determine whether the notched absorber maintained consistent performance despite polarisation changes. As depicted in Figure 12, the simulated results demonstrated that reflection coefficients remained stable across different polarization angles. It indicates that the notched absorber behaviour is unaffected by polarization variations, confirming its polarization-insensitive characteristics. Such consistency across varying polarization angles is highly desirable in applications where the orientation of incoming waves can vary or is unpredictable.

7.2. Oblique Incidence Results

Equations (2) and (3) define the reflection coefficients for the TE polarization ($(\Gamma_\perp)$) and TM polarization ($(\Gamma_\parallel)$) under the oblique incidence angle [17]:

$$\Gamma_\perp(\omega) = \frac{Z(\omega)\cos(\theta_i) - Z_o\cos(\theta_t)}{Z(\omega)\cos(\theta_i) + Z_o\cos(\theta_t)} \tag{2}$$

$$\Gamma_\parallel(\omega) = \frac{Z(\omega)\cos(\theta_i) - Z_o\cos(\theta_t)}{Z(\omega)\cos(\theta_i) + Z_o\cos(\theta_t)} \tag{3}$$

where θ_i, θ_t, $Z(\omega)$, and Z_o denote the angle of incidence, angle of transmission, an impedance of the notched absorber, and free space impedance, respectively. Figures 13 and 14 illustrate the

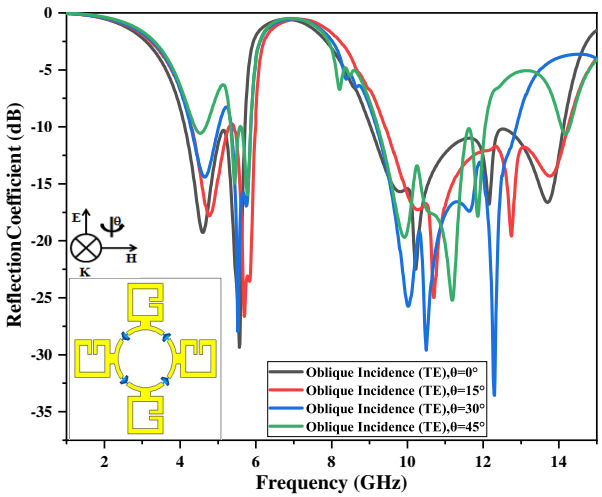

FIGURE 13. Simulated reflection coefficient of the proposed notched absorber for TE polarization under oblique incidence.

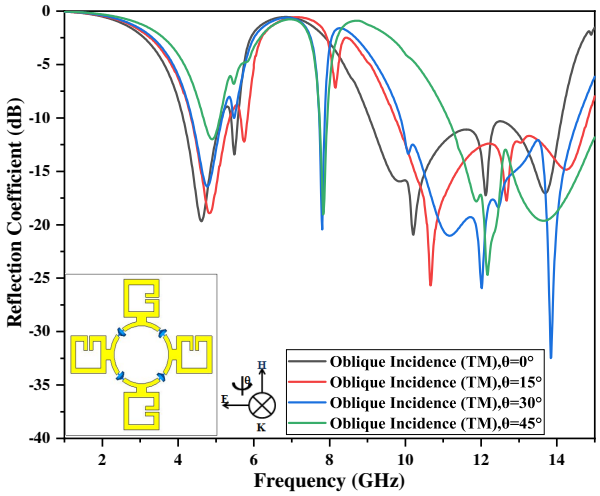

FIGURE 14. Simulated reflection coefficient of the proposed notched absorber for TM polarization under oblique incidence.

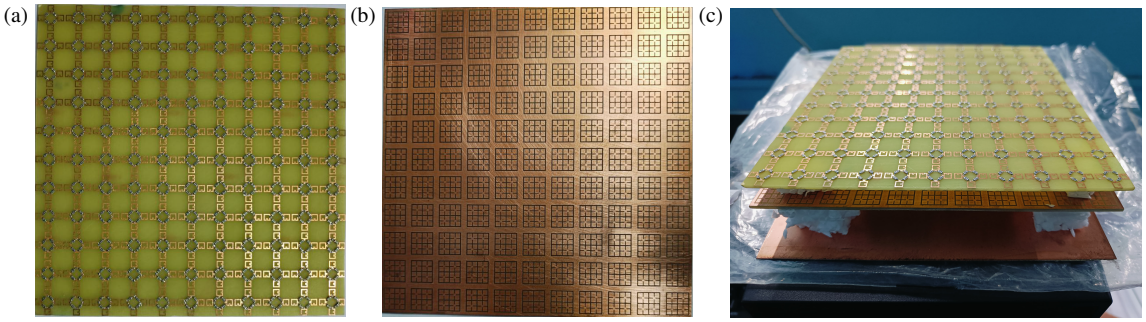

FIGURE 15. Fabricated proposed notched absorber. (a) Top layer. (b) Middle layer. (c) Side view.

variation in the reflection coefficient for a variety of incident angles (θ_i) under electromagnetic waves with TE and TM polarizations. Figure 13 shows that the reflection coefficient for out-of-band operation does not change much as the angle of incidence goes up by 15°. It stays less than −10 dB for the given frequency range up to 45°, though. Despite a modest reduction in the insertion loss, the reflection window remains stable up to an incidence angle of 45°.

In the case of TM polarization, while increasing the angle of incidence the reflection coefficient in the out-of-band operation band decreases. The reflection coefficient for the in-band reflection window is divided into two parts for increasing incidence angle, but insertion loss is almost constant which is shown in Figure 14.

The air-space separating the top and middle FSS functions as a transmission line, and its length is sensitive to oblique incidence; consequently, oblique incidence alters the overall input impedance of the transmission line, affecting the rasorber's reflection and transmission coefficients.

8. PROTOTYPE FABRICATION AND VALIDATION

To validate the simulated design, all three layers were fabricated using PCB technology and assembled for free space measurement, and the 3.0 mm air gap between the top and middle layers and 9.0 mm between the middle and bottom layers are maintained using foam. For the ease of fabrication and measurement, FR4 of thickness 1.0 mm was taken to the top and middle layers. The 11 × 11 unit cell was taken to fulfil the requirement of 5λ lengths of the fabricated structure.

The fabricated structure, as illustrated in Figure 15, has an overall dimension of 165 mm by 165 mm and consists of 121 unit cells. Figures 16(a) and (b) respectively illustrate the enlarged views of the top and intermediate layer-fabricated samples. A schematic diagram of the measurement apparatus is depicted in Figure 17, and the reflection coefficient of the fab-

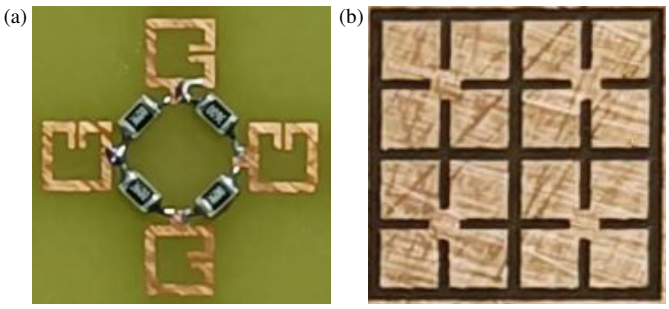

FIGURE 16. Enlarged view of the fabricated proposed notched absorber. (a) Top layer. (b) Middle layer.

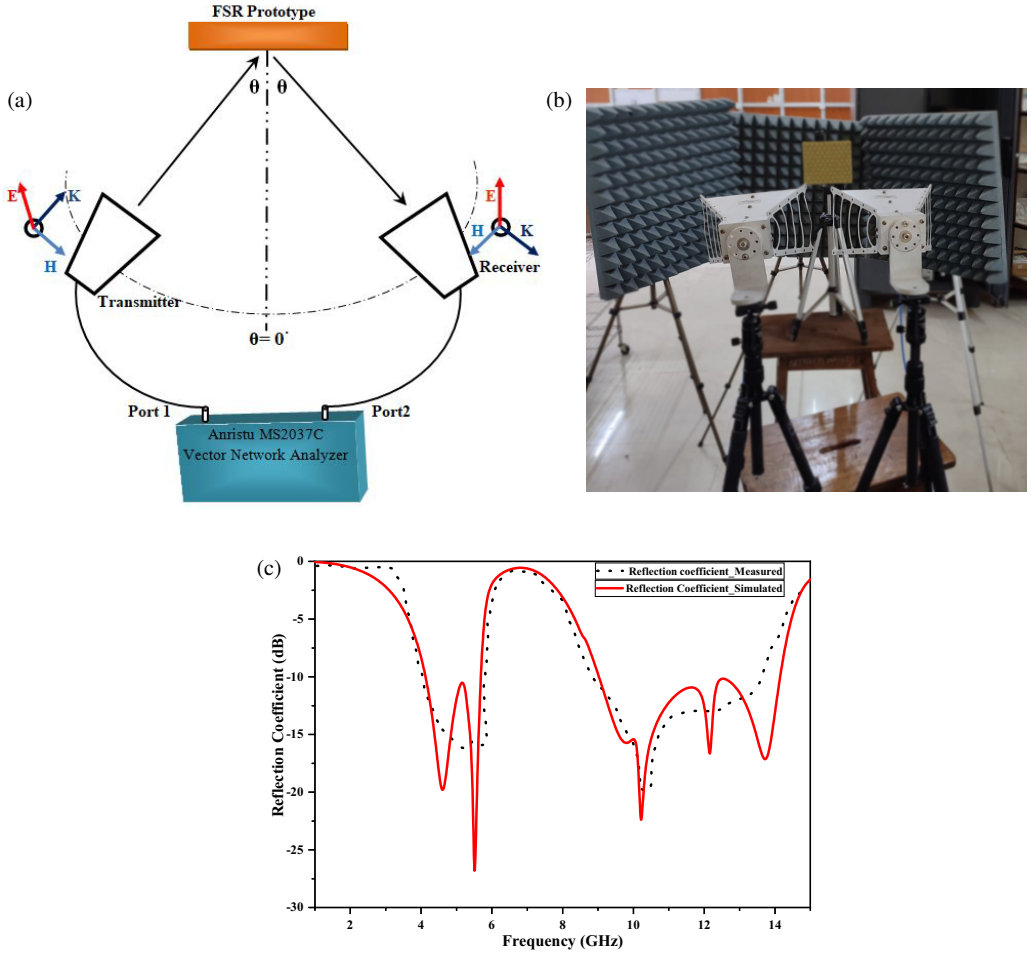

FIGURE 17. (a) Schematic diagram of the measurement setup for reflection coefficient. (b) Experimental setup for the measurement. (c) Comparison of simulated and measurement results of the proposed notched absorber.

TABLE 2. Comparison of the proposed rasorber with already published articles.

Ref.	Unit Cell Size (mm)	−3 dB Reflection Bandwidth	(Reflection Peaks) /IL (dB)	Angular Stability (Degrees) /Polarization Insensitive	(Fractional Bandwidth), (−3 dB Reflection Window) /(Overall Thickness)
[18]	15 (FR4) (Economical)	0.87 GHz	4.9 GHz/0.17 dB	40(TE), 40(TM) Yes	(130.5%)/(0.18λ)
[19]	25 (F4B) (costly)	1.6 GHz	3.5 GHz/0.12 dB	45(TE), 30(TM) Yes	(111.6%)/(0.22λ)
[20]	10.0 Duroid (Roger 5880), Costly	0.5 GHz	13.5 GHz/0.12 dB	50(TE), 40(TM) Yes	(112.0%)/(0.25λ)
[21]	25 (Teflon) (Costly)	0.41 GHz	3.54 GHz, 0.12 dB	30(TE), 30(TM) Yes	(95.4%)/(0.18λ)
[22]	16 (Rogers 4350B) $\tan\delta = 0.0037$ (Expensive)	0.54 GHz	7.41 GHz, 0.29 dB	45(TE), 45(TM) Yes	(111.5%), (0.22λ)
This Work	15 (FR4) (Economical)	2.2 GHz	6.80 GHz, 0.4 dB	45(TE), 45(TM) Yes	(110%)/(0.36λ)

ricated notched absorber was measured in an anechoic chamber. The Anritsu MS2037C Vector Network Analyser was hooked up to two horn antennas that worked in the frequency range of 2–18 GHz for the experiment. We employed these two horn antennas to transmit electromagnetic radiation and to receive the reflected power of the fabricated structure. We calibrated the network analyser using standard open-short-load (OSL) technology when we initially connected it to coaxial cables. We positioned small pyramidal absorbers between the two horn antennas to mitigate their coupling. The far-field requirements have been met by positioning the fabricated notched absorber at a sufficient distance from the antennas.

We first measured the reflection coefficient of a perfect reflector to eliminate the unwanted EM wave and propagation loss. Subsequently, we found the reflection coefficient by positioning the fabricated structure at the same location. The real reflection coefficient will be the difference between the two. Figure 17(c) compares the simulated and experimental test results. It shows an insertion loss of 0.45 dB at around 6.75 GHz and an absorptivity of over 80% from 4.0 GHz to 13.8 GHz.

Table 1 displays a comparison of the experimental and simulated results. Minor discrepancies between the experimental and simulated results are identified and could occur because the simulated result is for an infinite array of unit cells, whereas the fabricated sample is of a finite dimension. Furthermore, the measurement environment may differ from that of the simulation. Fabrication tolerances and instrument inaccuracies may also result in deviations.

Table 2 summarizes the comparisons between the proposed metamaterial notched absorber and other related notched absorbers currently available in the literature. The table illustrates that the proposed notched absorber offers a wide reflection bandwidth with low insertion loss, stable wide-angle absorption to both sides of the reflection window, and high relative bandwidth on the right side of the absorption spectra. The comparison table indicates that certain notched absorbers exhibit minimal insertion loss and thickness, but they use materials more expensive than FR4, leading to high manufacturing costs.

9. CONCLUSION

In this study, a novel notched absorber with a dual-polarized wide reflection window, polarization insensitivity, and high fractional bandwidth has been designed using CST software and validated through circuit analysis and experimental testing. The first out-of-band absorption bands extended from 4.1 GHz to 5.7 GHz, and the second absorption band spans from 9.0 GHz to 14.1 GHz. Between these two absorption bands a wide reflection window of -3 dB bandwidth of 2.2 GHz is observed around 6.8 GHz with the insertion loss of only 0.4 dB. The proposed notched absorber comprises three layers; the upper layer is equipped with lumped resistors to facilitate broadband absorption, while the middle layer is carefully engineered to work as a different filtering action for out-of-band absorption and in-band reflection operation. The bottom layer acts as a ground plane for the in-band reflection operation.

Given these features, the proposed notched absorber could be employed in various applications, such as radomes and electromagnetic compatibility solutions, to protect sensitive equipment from unwanted electromagnetic radiation like radio waves and microwaves. Moreover, when being used as a superstratum on an antenna, the notched absorber can contribute to reduced radar cross-section (RCS), enhancing stealth characteristics.

REFERENCES

[1] Salisbury, W. W., "Absorbent body for electromagnetic waves," US Patent No. 2599944 A, 1952.

[2] Chambers, B. and A. Tennant, "Design of wideband Jaumann radar absorbers with optimum oblique incidence performance," *Electronics Letters*, Vol. 30, No. 18, 1530–1532, 1994.

[3] Bucci, O. and G. Franceschetti, "Scattering from wedge-tapered absorbers," *IEEE Transactions on Antennas and Propagation*, Vol. 19, No. 1, 96–104, 1971.

[4] Munaga, P., S. Ghosh, S. Bhattacharyya, D. Chaurasiya, and K. V. Srivastava, "An ultra-thin dual-band polarization-independent metamaterial absorber for EMI/EMC applications," in *2015 9th European Conference on Antennas and Propagation (EuCAP)*, 1–4, Lisbon, Portugal, 2015.

[5] Ghosh, S., S. Bhattacharyya, Y. Kaiprath, D. Chaurasiya, and K. V. Srivastava, "Triple-band polarization-independent metamaterial absorber using destructive interference," in *2015 European Microwave Conference (EuMC)*, 335–338, Paris, France, 2015.

[6] Shelby, R. A., D. R. Smith, and S. Schultz, "Experimental verification of a negative index of refraction," *Science*, Vol. 292, No. 5514, 77–79, 2001.

[7] Cheng, Y., X. S. Mao, C. Wu, L. Wu, and R. Gong, "Infrared non-planar plasmonic perfect absorber for enhanced sensitive refractive index sensing," *Optical Materials*, Vol. 53, 195–200, 2016.

[8] Singh, D. and V. M. Srivastava, "An analysis of RCS for dual-band slotted patch antenna with a thin dielectric using shorted stubs metamaterial absorber," *AEU — International Journal of Electronics and Communications*, Vol. 90, 53–62, 2018.

[9] Kumari, B., A. Kumar, P. Kumar, and M. Singh, "Polarization independent ultra-wideband meta-material absorber using conductive ink resonator," *Journal of Telecommunications and Information Technology*, Vol. 1, No. 1, 39–45, 2024.

[10] Zheng, S., Y. Yin, J. Fan, X. Yang, B. Li, and W. Liu, "Analysis of miniature frequency selective surfaces based on fractal antenna-filter-antenna arrays," *IEEE Antennas and Wireless Propagation Letters*, Vol. 11, 240–243, 2012.

[11] Guo, Q., Z. Li, J. Su, L. Y. Yang, and J. Song, "Dual-polarization absorptive/transmissive frequency selective surface based on tripole elements," *IEEE Antennas and Wireless Propagation Letters*, Vol. 18, No. 5, 961–965, 2019.

[12] Huang, H., Z. Shen, and A. A. Omar, "3-D absorptive frequency selective reflector for antenna radar cross section reduction," *IEEE Transactions on Antennas and Propagation*, Vol. 65, No. 11, 5908–5917, 2017.

[13] Mei, P., X. Q. Lin, J. W. Yu, A. Boukarkar, P. C. Zhang, and Z. Q. Yang, "Development of a low radar cross section antenna with band-notched absorber," *IEEE Transactions on Antennas and Propagation*, Vol. 66, No. 2, 582–589, 2017.

[14] Jenn, D., *Radar and Laser Cross Section Engineering*, 2nd ed., American Institute of Aeronautics and Astronautics, Inc., USA, 2005.

[15] Kumar, A., G. Sen, and J. Ghosh, "Design of a compact SRR loaded polarization-independent wideband meta-material rasorber with a narrow transmission window," *Progress In Electromagnetics Research M*, Vol. 131, 37–44, 2025.

[16] Sambhav, S., J. Ghosh, and A. K. Singh, "Ultra-wideband polarization insensitive thin absorber based on resistive concentric circular rings," *IEEE Transactions on Electromagnetic Compatibility*, Vol. 63, No. 5, 1333–1340, 2021.

[17] Kumar, A. and J. Ghosh, "Polarization-independent wideband meta-material absorber based on resistor-loaded hexagonal ring resonators," *Journal of Electromagnetic Waves and Applications*, Vol. 38, No. 2, 264–281, 2024.

[18] Sambhav, S. and J. Ghosh, "A miniaturized dual-polarized band notched absorber with low insertion loss," *Progress In Electromagnetics Research M*, Vol. 112, 231–241, 2022.

[19] Mei, P., X. Q. Lin, J. W. Yu, and P. C. Zhang, "A band-notched absorber designed with high notch-band-edge selectivity," *IEEE Transactions on Antennas and Propagation*, Vol. 65, No. 7, 3560–3567, 2017.

[20] Kumar, A., J. B. Padhi, R. Jawale, and G. S. Reddy, "A frequency selective surface based polarization-independent band notched electromagnetic (EM) wave absorber," in *2023 XXXVth General Assembly and Scientific Symposium of the International Union of Radio Science (URSI GASS)*, 1–4, Sapporo, Japan, 2023.

[21] Han, Y., L. Zhu, Y. Chang, and B. Li, "Dual-polarized bandpass and band-notched frequency-selective absorbers under multimode resonance," *IEEE Transactions on Antennas and Propagation*, Vol. 66, No. 12, 7449–7454, 2018.

[22] Li, Z., G. Zhang, S. Yang, Y. Lun, Z. Che, J. Yue, and J. Suo, "Dual-polarized frequency selective absorber with in-band reflection response," *Microwave and Optical Technology Letters*, Vol. 64, No. 10, 1740–1745, 2022.